

**Ting Zhu**

Department of Mechanical Engineering,  
Massachusetts Institute of Technology,  
Cambridge, MA 02139

**Ju Li**

Department of Materials Science and  
Engineering,  
Ohio State University,  
Columbus, OH 43210

**Sidney Yip**

Departments of Nuclear Engineering and  
Materials Science and Engineering,  
Massachusetts Institute of Technology,  
Cambridge, MA 02139  
e-mail: syip@mit.edu

# Nanomechanics of Crack Front Mobility

*Minimum energy paths for unit advancement of a crack front are determined by reaction pathway sampling, thus providing the reaction coordinates for the analysis of crack tip mechanics in ductile and brittle materials. We compare results on activation energy barrier and atomic displacement distributions for an atomically sharp crack in Cu, where one observes the emission of a partial dislocation loop, and in Si, where crack front extension evolves in a kink-like fashion. [DOI: 10.1115/1.2047607]*

## 1 Introduction

Is it possible to study how a sharp crack evolves in a crystal lattice without actually driving the system to the point of instability? By this we mean determining the pathway of crack front motion while the lattice resistance against such displacement is still finite. Despite a large number of molecular dynamics (MD) simulations on crack tip propagation (e.g., see [1]), this particular issue has not been examined. Most studies to date have been carried out in an essentially 2D setting, with a periodic boundary condition imposed along the direction of the crack front. In such simulations the crack tip is sufficiently constrained that the natural response of the crack front cannot be investigated. Besides the size constraint on the crack front, there is also the problem that in direct MD simulation one frequently drives the system to instability, resulting in abrupt crack-tip displacements which make it difficult to characterize the slow crack growth by thermal activation.

We have developed an approach capable of probing crack front evolution without subjecting the system to critical loading. This involves using reaction pathway sampling to probe the minimum energy path (MEP) [2] for the crack front to advance by one atomic lattice spacing, while the imposed load on the system is below the critical threshold. We have applied this method to characterize the atomistic configurations and energetics of crack extension in a metal (Cu) [3] and a semiconductor (Si) [4]. In this report we will compare the results of these two studies to show how ductility or brittleness of the crystal lattice can manifest in the mechanics of crack front deformation at the nanoscale.

Consider a 3D atomically sharp crack front which is initially straight, as shown in Fig. 1(a). Suppose we begin to apply a mode-I load in incremental steps. Initially the crack would not move spontaneously because the driving force is not sufficient to overcome the intrinsic lattice resistance. What does this mean? Imagine a final configuration, a replica of the initial configuration with the crack front translated by an atomic lattice spacing in the direction of crack advancement. At low loads, e.g.,  $K_I^*$  as shown in Fig. 1(b), the initial configuration (open circle) has a lower energy than the final configuration (closed circle). They are separated by

an energy barrier which represents the intrinsic resistance of the lattice. As the loading increases, the crack will be driven toward the final configuration; one can regard the overall energy landscape as being tilted toward the final configuration with a corresponding reduction in the activation barrier [see the saddle-point states (shaded circle) in Fig. 1(b)]. As the load increases further the biasing becomes stronger. So long as the barrier remains finite the crack will not move out of its initial configuration without additional activation, such as from thermal fluctuations. When the loading reaches the point where the lattice-resistance barrier disappears altogether, the crack is then unstable at the initial configuration; it will move without any thermal activation. This is the athermal load threshold, denoted by  $K_{Iath}$  in Fig. 1(b). In our simulation, we study the situation where the applied load is below this threshold, thereby avoiding the problem of a fast moving crack that is usually over-driven.

The cracks in Cu and Si that we will compare are both semi-infinite cracks in a single crystal, with the crack front lying on a (111) plane and running along the  $[\bar{1}10]$  direction. The simulation cells consist of a cracked cylinder cut from the crack tip, with a radius of 80 Å. The atoms located within 5 Å of the outer surface are fixed according to a prescribed boundary condition, while all the remaining atoms are free to move. To probe the detailed deformation of the crack front, the simulation cell along the cylinder is taken to be as long as computationally feasible, 24 (Cu) and 20 (Si) unit cells. A periodic boundary condition is imposed along this direction. With this setup, the numbers of atoms in the system are 103,920 (Cu) and 77,200 (Si). For interatomic potentials we use a many-body potential of the embedded atom method type for Cu [5], for which the unstable stacking energy has been fitted to the value of 158 mJ/m<sup>2</sup>, given by an ab initio calculation, and a well-known three-body potential model proposed by Stillinger and Weber (SW) for Si [6].

## 2 MEP for Crack Blunting in Cu

Prior to applying reaction pathway sampling, we first determine the athermal energy release rate, denoted by  $G_{emit}$  [corresponding to  $K_{Iath}$  in Fig. 1(b)]. This is the critical value at which the activation energy barrier for dislocation nucleation vanishes, or equivalently a straight dislocation is emitted without thermal fluctuations [7,8]. As detailed in [3], the athermal load is determined to be  $K_{Iemit}=0.508 \text{ MPa}\sqrt{\text{m}}$  (or  $G_{emit}=1.629 \text{ J/m}^2$  based on the Stroh solution [9]) for the nucleation of a Shockley partial dislocation across the inclined ( $\bar{1}10$ ) slip plane. So long as the applied load is below  $K_{Iemit}$  the crack front will remain stable. It is in such

Contributed by the Applied Mechanics Division of THE AMERICAN SOCIETY OF MECHANICAL ENGINEERS for publication in the ASME JOURNAL OF APPLIED MECHANICS. Manuscript received by the Applied Mechanics Division, October 5, 2004; final revision, October 5, 2005. Review conducted by H. D. Espinosa. Discussion on the paper should be addressed to the Editor, Prof. Robert M. McMeeking, Journal of Applied Mechanics, Department of Mechanical and Environmental Engineering, University of California—Santa Barbara, Santa Barbara, CA 93106-5070, and will be accepted until four months after final publication in the paper itself in the ASME JOURNAL OF APPLIED MECHANICS.

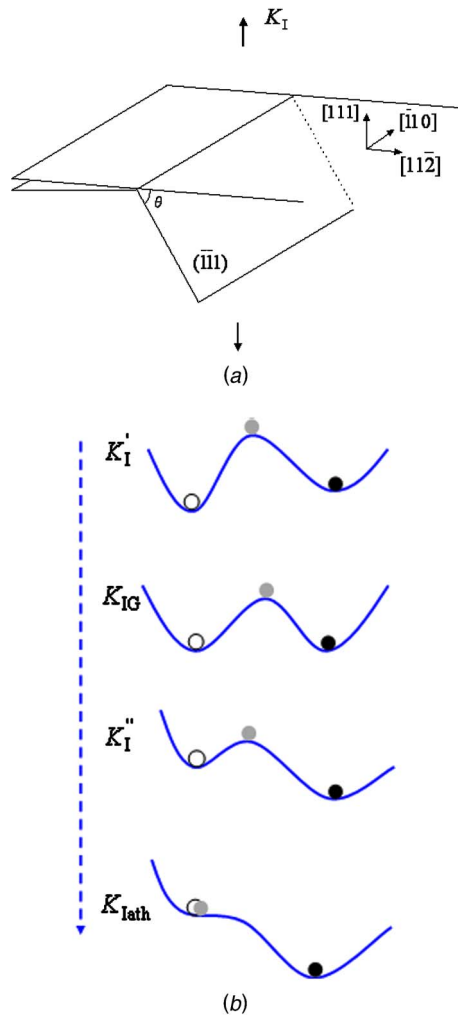


**Fig. 1** (a) Schematics of a 3D atomically sharp crack front under a mode-I load  $K_I$ ; (b) energy landscape of the crack system at different loads ( $K'_I < K_{IG} < K''_I < K_{lath}$ ). Open circle represents the initial state of a straight crack front under an applied load  $K_I$ , closed circle is the final state after the crack front uniformly advances by one atomic spacing (under the same load  $K_I$  as the initial state), and shaded circle corresponds to the saddle-point state in between.

a state that we will probe the reaction pathway for dislocation nucleation using the method of nudged elastic band (NEB) [2]. The quantity we wish to determine is the MEP for the emission of a partial dislocation loop from an initially straight crack front. MEP is a series of atomic configurations connecting the initial and final states. For this study the initial configuration is a crack front as prescribed by the Stroh solution which is then relaxed by energy minimization. The final configuration contains a fully formed straight Shockley partial dislocation at the same level of loading as the initial state. This is obtained by first loading the simulation cell at a level above the threshold  $G_{emit}$  so that a partial dislocation could instantaneously nucleate. Then the loading is reduced to the level of the initial state (below  $G_{emit}$ ) thus generating a configuration with an embedded partial dislocation. To find the MEP 15 intermediate replicas of the system which connect the initial and final states are constructed. We choose intermediate replicas containing embryonic loops that result from the relaxation of a straight crack front, allowing for the nucleation of a curved dislocation. The relaxation of each replica is considered converged when the potential force vertical to the path is less than a prescribed value,  $0.005 \text{ eV/\AA}$  in our case.

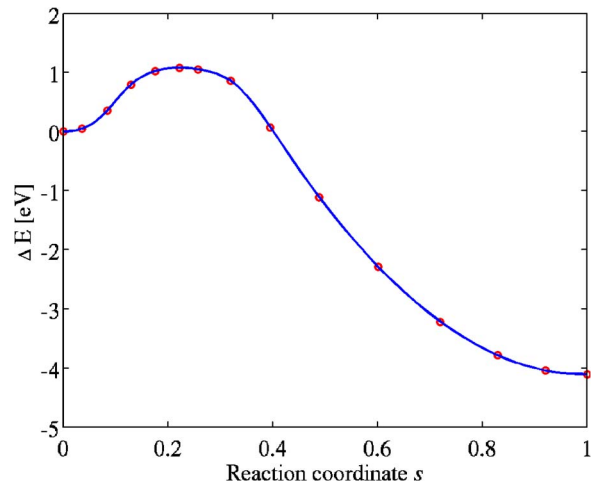


**Fig. 2** MEP of dislocation loop emission in Cu at a load of  $G = 0.75 G_{emit}$  [3]

The sequence of replicas defines a reaction coordinate in the following sense. Each replica in the sequence is a specific configuration in  $3N$  configurational hyperspace, where  $N$  is the number of movable atoms in the simulation. For each replica we calculate the hyperspace arc length  $l$  between the initial state  $x_i^{3N}$  and the state of the replica  $x^{3N}$ . The normalized reaction coordinate  $s$  is defined to be  $s \equiv l/l_f$ , where  $l_f$  denotes the hyperspace arc length between the initial and final states.

The relaxed energy of any replica is a local minimum within a  $3N-1$  hyperplane vertical to the path. By definition the MEP is a path that begins at  $\Delta E=0 (s=0)$ , where  $\Delta E$  is the relaxed energy measured relative to the energy of the initial state. Along the path (reaction coordinate  $s$ )  $\Delta E$  will vary. The state with the highest energy on this path is the saddle point, and the activation energy barrier is the energy difference between the saddle point and the initial state. Figure 2 shows the MEP for the nucleation of a dislocation loop from the crack front in Cu, loaded at  $G=0.75 G_{emit}$ . Notice that at this loading the final state is strongly favored over the initial state. Figure 2 shows clearly the presence of a lattice-resistance barrier at this particular loading.

To visualize the variation of atomic configurations along the MEP, we turn to displacement distributions between atom pairs across the slip plane. Figure 3(a) is a contour plot of the shear displacement distribution along the crack front at the saddle-point state. One can see clearly the shape of a dislocation loop bowing out; the profile of  $b/2$  shear displacement is a reasonable representation of the locus of dislocation core. Also this is an indication that the enclosed portion of the crack front has been swept by the Shockley partial dislocation loop. Besides shear displacement, normal, or opening displacement, in the direction along  $x_3, [\bar{1}\bar{1}1]$ , is also of interest. The corresponding distribution is shown in Fig. 3(b). One sees that large displacements are not at the center of the crack front. In Figs. 3(a) and 3(b) we have a detailed visualization of the crack front evolution in three dimensions. The largest displacements are indeed along the crack front but they are not of the same character; the atoms move in a shear mode in the central region and in an opening mode on the two sides.

### 3 MEP for Crack Advancement in Si

Turning to Si, we first repeat the determination of athermal load for crack extension in the (111) plane;  $K_{lath}=0.88 \text{ MPa}\sqrt{\text{m}}$ . Since Si is a brittle solid, a useful reference load is  $K_{IG}$ , the Griffith value at which the initial and final states are at the same energy [see Fig. 1(b)], the latter being identical to the initial state except the crack front advances one atomic spacing in the propagation

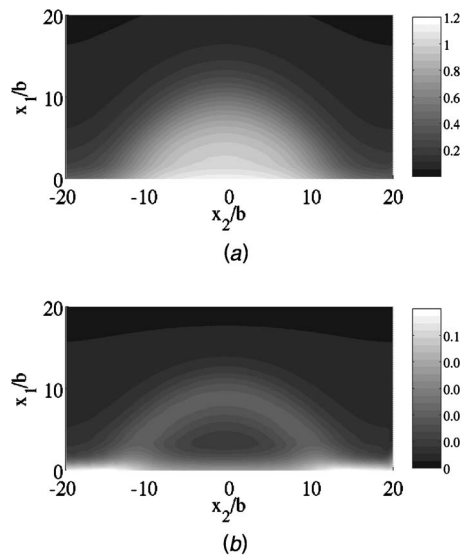


**Fig. 3 Contour of (a) shear displacement (normalized by the Burgers vector of a partial dislocation  $b=1.476 \text{ \AA}$ ) and (b) opening displacement (normalized by the interplanar spacing  $h=2.087 \text{ \AA}$ ) across the slip plane at the saddle-point state [3]**

direction. Direct simulation gives  $K_{IG}=0.646 \text{ MPa}\sqrt{\text{m}}$ . This value is lower than the athermal load  $K_{Iath}$ , a manifestation of the lattice-trapping effect [10]. Being a brittle solid, the relevant deformation in crack front advancement in Si is bond rupture rather than bond shearing as in the case of a ductile material such as Cu. Our simulation cell contains 20 bonds along the initially straight crack front. We find that the most energetically favored pathway for the front to advance by one atomic spacing is the breaking of the 20 bonds *sequentially*. At a load equal to the Griffith value, the MEP we obtain is shown in Fig. 4. A slightly different reaction coordinate is used in this case, with integer  $s$  labeling a locally equilibrated state with  $s$  broken bonds on the crack front. One sees the energy variation is a series of barriers, each one corresponding to the rupture of a bond along the crack front.

Figure 5 shows the opening displacement distribution in Si across the (111) cleavage plane. We see a new feature in the outline of displacements of intermediate magnitude (dark-gray line); in the region ahead of the crack front the distribution of these displacements has the shape of a rectangular wedge protruding in the direction of crack front advancement. The presence of a wedge shape suggests a kink mechanism of crack advancement, namely,

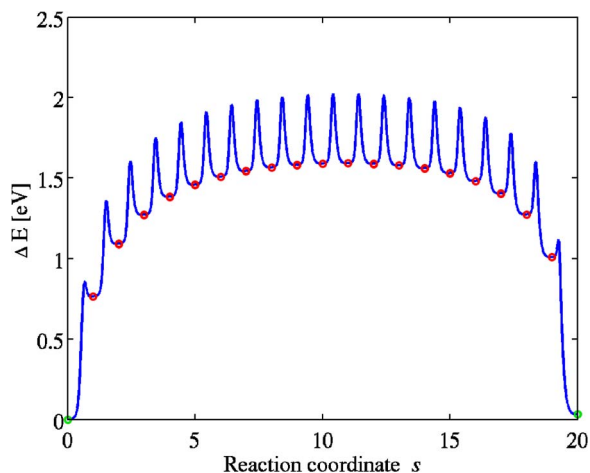


**Fig. 4 MEP of crack extension in Si at the Griffith load  $K_{IG}$  [4]**

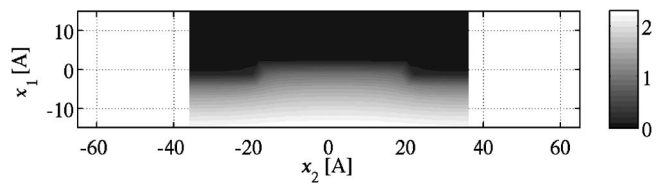


**Fig. 5 Contour of opening displacement (normalized by interplanar spacing  $h=2.35 \text{ \AA}$ ) at the Griffith load  $K_{IG}$  [4]**

nucleation of a local kink distortion followed by spreading across the entire crack front. It is significant that this behavior is not seen in Fig. 3(b). Taking Cu to be a prototypical ductile material, we see that while the crack opening still occurs at the front, the large normal displacements lie outside the central region enclosed by the emerging dislocation loop. We attribute this feature to a mode-switching, or shear-tension coupling, process. The initially large opening displacements in the region swept by the emerging loop are relaxed by giving way to large shear displacements, which are then carried away by the emitted dislocation loop.

It is relevant to interpret the behavior of atomic displacements at the transition state in Cu and Si on the basis of the nature of interatomic bonding in these two materials. One expects that the crack front response in Cu should reflect delocalized metallic bonding while that in Si should correspond to directional, localized covalent bonding. In terms of characteristic features of the energy landscape along the reaction path, we see for Cu (in Fig. 2) a rather smooth MEP with a single major nucleation barrier, indicating that crack advancement involves a concerted motion of atoms to overcome this barrier by thermal activation. In contrast MEP in Si reveals the existence of significant secondary barrier (cusps in Fig. 4) which should be a general feature of covalently bonded crystals. In this case crack extension proceeds via individual bond breakings, a series of thermally activated events of kink-pair formation, and lateral kink migration along the front. It is of interest to point out the crack front mobility is not only controlled by kinks at the atomic scale as demonstrated in this work; acoustic emission and fractographic measurements have indicated the crack advancement at the mesoscopic scale is also governed by the kink mechanism which involves a process of unzipping along the crack front (W. W. Gerberich, private communication; [11]).

The fact that kink mechanism appears to play a central role in crack front mobility raises an interesting question of the implications of structural similarity between the crack front, acting as the core of a sharp crack, and the core of a dislocation, both being “line defects” in a crystal lattice. It is rather well known that dislocation mobility in a directionally bonded crystal like Si is governed by thermal activation of nucleation and migration of kink pairs [12]. The present results showing that a similar mechanism also operates in crack front advancement reinforces the notion that mobility fundamentally depends on crystal structure and chemical bonding. From this perspective the appearance of kink-like structure in Fig. 5 is perhaps to be expected. Since dislocation mobility and crack-tip extension are both active topics for modeling and simulation, recognition of their underlying connections could lead to a broader appreciation of the role of structure and bonding [13] in controlling both phenomena.

## Acknowledgments

We thank A. S. Argon for stimulating discussions and W. W. Gerberich for a useful reference. TZ and SY acknowledge support by NSF, Honda R&D, DARPA-ONR, and the Lawrence Livermore National Laboratory. JL acknowledges support by Honda Research Institute of America, NSF, AFOSR, ONR, and Ohio Supercomputer Center.

## References

- [1] Buehler, M. J., Abraham, F. F., and Gao, H., 2003, "Hyperelasticity Governs Dynamic Fracture at a Critical Length Scale," *Nature (London)*, **426**, pp. 141–146.
- [2] Jonsson, H., Mills, G., and Jacobsen, K. W., 1998, "Nudged Elastic Band Method for Finding Minimum Energy Paths of Transitions," *Classical and Quantum Dynamics in Condensed Phase Simulations*, B. J. Berne, G. Ciccotti, and D. F. Coker, eds., World Scientific, Singapore, pp. 385–404.
- [3] Zhu, T., Li, J., and Yip, S., 2004, "Atomistic Study of Dislocation Loop Emission From a Crack Tip," *Phys. Rev. Lett.*, **93**, 025503.
- [4] Zhu, T., Li, J., and Yip, S., 2004, "Atomic Configurations and Energetics of Crack Extension in Silicon," *Phys. Rev. Lett.*, **93**, 205504.
- [5] Mishin, Y., Mehl, M. J., Papaconstantaopoulos, D. A., Voter, A. F., and Kress, J. D., 2001, "Structural Stability and Lattice Defects in Copper: *Ab initio*, Tight-Binding, and Embedded-Atom Calculations," *Phys. Rev. B*, **63**, 224106.
- [6] Stillinger, F. H., and Weber, T. A., 1985, "Computer Simulation of Local Order in Condensed Phases of Silicon," *Phys. Rev. B*, **31**, pp. 5262–5271.
- [7] Rice, J. R., 1992, "Dislocation Nucleation From a Crack Tip: An Analysis Based on the Peierls Concept," *J. Mech. Phys. Solids*, **40**, pp. 239–271.
- [8] Xu, G., Argon, A. S., and Ortiz, M., 1997, "Critical Configurations for Dislocation Nucleation From Crack Tips," *Philos. Mag. A*, **75**, pp. 341–367.
- [9] Stroh, A. N., 1958, "Dislocations and Cracks in Anisotropic Elasticity," *Philos. Mag.*, **7**, pp. 625–646.
- [10] Thomson, R., Hsieh, C., and Rana, V., 1971, "Lattice Trapping of Fracture Cracks," *J. Appl. Phys.*, **42**, pp. 3145–3160.
- [11] Lii, M. J., Chen, X. F., Katz, Y., and Gerberich, W. W., 1990, "Dislocation Modeling and Acoustic-Mission Observation of Alternating Ductile/Brittle Events in Fe-3 wt% Si Crystals," *Acta Metall. Mater.*, **38**, pp. 2435–2453.
- [12] Cai, W., Bulatov, V. V., Chang, J., Li, J., and Yip, S., 2004, "Dislocation Core Effects on Mobility," in *Dislocations in Solids*, F. R. N. Nabarro and J. P. Hirth, eds., Elsevier, Amsterdam, Vol. 12, Chap. 64, pp. 1–80.
- [13] Ogata, S., Li, J., Hirotsaki, N., Shibutani, Y., and Yip, S., 2004, "Ideal Shear Strain of Metals and Ceramics," *Phys. Rev. B*, **70**, pp. 104104.